Structure and Chemical Activity of Point Defects on $MgCl_2$ (001) Surface

Karine Costuas[†,‡] and Michele Parrinello*[,†,‡]

Max-Planck-Institut für Festkörperforschung, Heisenbergstrasse 1, D-70569 Stuttgart, Germany; CSCS−Swiss Center for Scientific Computing, Via Cantonale, CH-6928 Manno, Switzerland; Department of Physical Chemistry, ETH, Hönggerberg HCI, CH-8093 Zurich, Switzerland

Received: November 15, 2001; In Final Form: February 15, 2002

$MgCl_2$ is a support of choice for industrial production of polyolefins in Ziegler−Natta catalysis. Recent experiments have shown that the inert (001) $MgCl_2$ surface can be activated by electron irradiation. To better understand this process, we have studied the properties of point defects on the (001) surface and their interaction with $TiCl_4$. We have used density functional theory and Car−Parrinello methods and calculated mono- and di-vacancies of Cl and Cl^-. Particularly interesting is the case of Cl di-vacancy which is heavily reconstructed and forms with $TiCl_4$ a structure where the Ti atom is bounded with a Mg atom.

Introduction

Knowledge of the structure and composition of the active sites in the Ziegler−Natta catalyst ($MgCl_2/TiCl_4$)[1] and the understanding of the catalytic process are both crucial to improve its activity. However, despite intensive experimental[2] and theoretical[3,4] researches, our present understanding is incomplete. Many unanswered questions remain, not least the formation and structure of the active sites. Indeed, there is strong evidence for a multiplicity of sites whose nature is still undetermined. Microscopic determination of these sites is difficult because many surface science experimental probes do not work on insulating surfaces.[5] Each center has its own distinctive properties and only a small percentage of the Ti site is active.

It would, however, be very desirable to have control and understanding of these sites. In such a way one could tune the properties of the polymer by modifying the nature of the catalytic center. To this effect, Somorjai et al. chose to work on a well-defined surface model, viz., $MgCl_2$ (001),[6−15] although it is believed that the most relevant surfaces are (110) and (111) in the industrial catalyst. The $MgCl_2$ crystal has a layer structure and the (001) surface is the cleavage surface. This makes it ideal for surface science studies.

However, the (001) surface is chemically inert and needs to be activated. To achieve this result, Somorjai et al. irradiated it with electrons. In doing this, they assume that surface defects are created upon irradiation, including pairs of F-centers (two nearby Cl vacancies occupied by electrons) and H-centers, i.e., molecular halogen anions in lattice position.[11] They highlighted by Auger electron spectroscopy the presence of reduced Mg atoms exposed at the surface. After irradiation, they observed a complex phenomenology as a function of the deposition procedure of $TiCl_4$.

Inspired by this work and also by the consideration that during the exothermic catalytic process defects can be generated on the (001) $MgCl_2$ surface, we have studied a variety of surface defects. We have also investigated the fact that on these defects, a $TiCl_4$ molecule can be absorbed, possibly leading to the formation of interesting catalytic centers.

Our theoretical work is based on density functional theory (DFT) as implemented in the Car−Parrinello method. We found a variety of defects, some of which imply a large local relaxation. We also considered the possibility that a $TiCl_4$ molecule could be adsorbed on these defects. These calculations show that the defective surface is highly reactive. Particularly interesting is the case in which a $TiCl_4$ molecule is made to interact with a $Cl^{\cdot}$ di-vacancy. In this case, there was a strong rearrangement and one Mg atom had moved to the top of the layer and formed an intermetallic bond with the Ti center.

1. Computational Details

We performed DFT calculations[16] using the Becke−Lee−Yang−Parr (BLYP)[17] approximation to the exchange and correlation functionals. We expanded the Kohn−Sham orbitals in plane waves up to a cutoff energy of 40 Rydberg. We used periodic boundary conditions and a trigonal supercell of size $a = 10.95$ Å, $c = 27.51$ Å. We considered only one $MgCl_2$ layer, since the interaction between layers is weak. The cell contains 9 chemical units. This size is such that the interactions between the repeated layers in the *c* direction can be neglected as well as the intralayer interactions between defect images.

We used the soft norm conserving pseudopotentials of Trouiller and Martins,[18] and we included nonlinear core corrections[19] for Mg and Ti. Only the Γ point of the Brillouin zone was sampled. For the open-shell systems, we performed spin-unrestricted calculations. In the case of charged systems, a compensating uniform background was introduced in order to restore charge neutrality. The results presented were obtained with the CPMD code.[20] The theoretical scheme employed has been used successfully in previous studies.[4] The cell dimensions used here correspond to the theoretical equilibrium structure and are in good agreement with the experimental ones ($a = 3.64$ Å).[21] In the theoretical structure, the Mg−Cl bonds are 2.53 Å and the Mg−Mg distances are 3.65 Å.

2. Surface Defects

The relevant crystal structure is α-$MgCl_2$, a layered crystal structure that belongs to the *R*3*m* space group. Each layer is

* Corresponding author. Fax: +41 91 610 83 08. E-mail: parrinello@cscs.ch.
† Max-Planck-Institut für Festkörperforschung.
‡ Present address: CSCS, Manno, Switzerland.

10.1021/jp014216e CCC: $22.00
Published on Web 04/06/2002

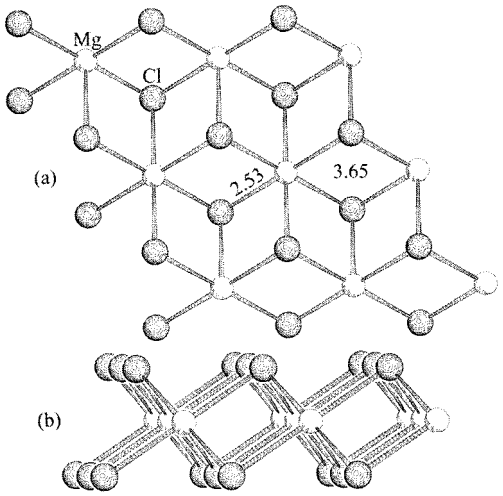

Figure 1. Relaxed $MgCl_2$ (001) monolayer. (a) *ab* plane. (b) *ac* plane. Distances are given in Å.

composed of 6-fold Mg atoms and 3-fold Cl atoms. The Mg−Cl interactions are ionic. These layers interact via van der Waals forces along the *c* axis. This structure has been previously studied by means of DFT calculations, with good agreement with experimental data.[4a] As explained before, this work focuses on the (001) surface, the basal plane of the α-$MgCl_2$ crystal. This surface is relatively easy to obtain, since only van der Waals interactions are involved in the cohesion between layers along the (001) axis.

The cleavage of the $MgCl_2$ crystal perpendicularly to the (001) axis leads to a surface that is completely saturated; the structural arrangement within the surface is therefore unchanged compared to the one within a layer of the bulk (see Figure 1).

This surface is catalytically inactive, each magnesium atom being in the Mg^{II} oxidation state and each Cl atom being formally a Cl^- ion. We explicitly verified this point by placing a $TiCl_4$ molecule close to the $MgCl_2$ surface and performing a Car−Parrinello (CP) molecular dynamic[22] simulation at 330 K. As expected, and in agreement with experiment, no reaction was observed.

We therefore examined the surface properties when Cl and Cl^- mono- and di-vacancies were created. Since we are interested in the exposed surface and experimentally the electron beam affects the top of the surface, only Cl atoms from the upper part of the layer were removed.

2.1. Cl^- Vacancy. By removing a Cl^- ion, the system relaxed as one would expect in such a cationic system, namely, the three undercoordinated Mg^{2+} moved outward with a displacement of 0.34 Å from the equilibrium position. Consequently, their distances with the Cl atoms in the apical position of the defect site were shortened from 2.53 to 2.37 Å. The Mg−Cl bond distances in the equatorial position of the defect were also shortened to 2.46 Å for the one surrounding the defect, and to 2.49 Å for the two others. The optimized structure is shown Figure 2. The total energy gain by this relaxation process is 63.9 kcal/mol, the formation energy is −102.9 kcal/mol.

2.2. Cl^- Di-vacancy. We removed two Cl^- neighboring ions. The resulting relaxed geometry is shown in Figure 3. The two geometries of the defects are symmetric. The changes occurring in the coordination sphere of Mg(1), Mg(2), Mg(4), and Mg(5) by relaxation are similar. For those atoms, there is a shortening of the Mg−Cl distance in the apical position of the defects to 2.42 Å, and a shortening of one Mg−Cl distance over two in

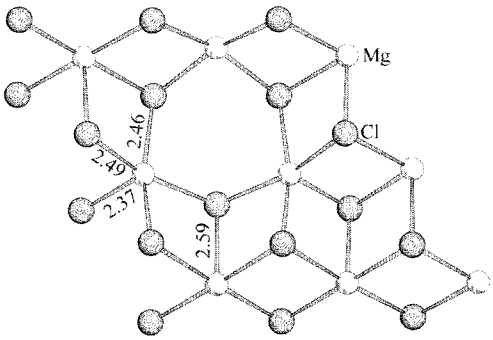

Figure 2. Relaxed $MgCl_2$ (001) monolayer with a Cl^- mono-vacancy (*ab* plane). The major structural changes upon relaxation are indicated. Bond lengths are expressed in Å. Other distances can be obtained by symmetry considerations since the vacancy has a C_3 symmetry axis. Relaxation energy = 63.9 kcal/mol.

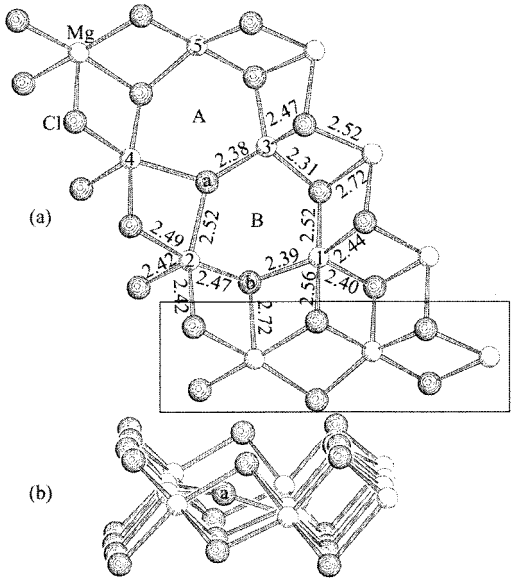

Figure 3. Relaxed $MgCl_2$ (001) monolayer with a Cl^- di-vacancy. The major structural changes upon relaxation are indicated. (a) *ab* plane. (b) *ac* plane. Distances are given in Å. Other distances can be obtained by symmetry considerations: symmetry plane formed by Mg(3), Cl(a), and the middle of Mg(2)−Mg(4)). A and B correspond to the position of the removed atoms. Relaxation energy = 17.5 kcal/mol per defect.

the equatorial position. The Mg(3) atom is in a distorted tetrahedral environment, as shown Figure 3. Cl(a) near the two defects has a quasi-planar Mg environment. The gain in energy of this relaxation process is 17.5 kcal/mol per defect, the energy needed to form this defect is −252.5 kcal/mol.

2.3. $Cl^\bullet$ Vacancy. The removal of a $Cl^\bullet$ atom from the $MgCl_2$ (001) surface leads to the formation of an F-center where one unpaired electron replaces a Cl^- in the $MgCl_2$ structure. The geometrical changes are small but significant, with an energy gain of 32.4 kcal/mol. The formation energy is −222.4 kcal/mol. The most stable geometrical configuration breaks the C_3 symmetry of the site and the Mg atoms moved further inward, shortening their distances from 3.65 Å to 3.54, 3.54, and 3.59 Å. A geometry relaxation with a C_3 symmetry constraint was only 0.2 kcal/m higher in energy. For this distortion, we cannot invoke Jahn−Teller effects since there are no degenerate levels that are partly occupied.[23] The distortion can be seen as due to a Coulomb energy gain that slightly overcomes the increase in the F electron quantum kinetic energy.

We visualize the F-center electron by use of its Wannier function. Wannier functions can be seen as an extension to the

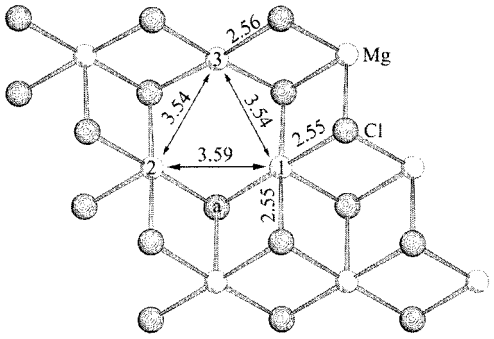

Figure 4. Relaxed $MgCl_2$ (001) monolayer with a $Cl^{\cdot}$ mono-vacancy (*ab* plane). The major structural changes upon relaxation are indicated. Bond lengths are expressed in Å. Other distances can be obtained by symmetry considerations: symmetry plane formed by Mg(3), Cl(a), and the middle of Mg(1)−Mg(2)). Relaxation energy = 32.4 kcal/mol.

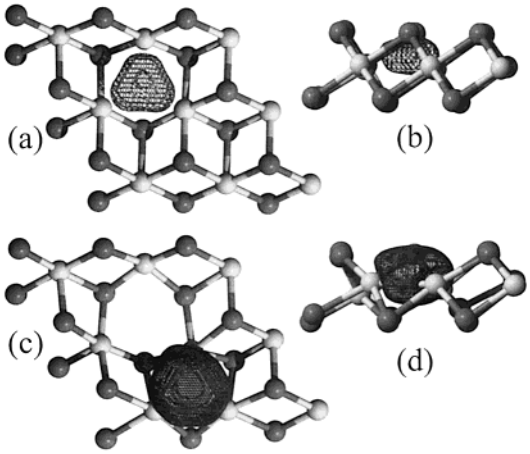

Figure 5. Contour plot of Wannier functions of $Cl^{\cdot}$ mono-vacancy $MgCl_2$ (001) F-center in (a) *ab* plane and (b) *ac* plane and of $Cl^{\cdot}$ di-vacancy $MgCl_2$ (001) F^--center in (c) *ab* plane and (d) *ac* plane. Contour values are 0.2 $(e/bohr^3)^{1/2}$.

periodic systems of the Boys localized orbitals.[24] The F-center Wannier function is localized at the vacancy and its wave function extends outward into the vacuum (see Figure 5a).

2.4. $Cl^{\cdot}$ Di-vacancy. The behavior of the two neighboring $Cl^{\cdot}$ vacancies is rather interesting. In fact, the two F-centers are unstable and two different defects are formed. An electron is removed from one vacancy, leaving behind a charged Cl vacancy (A of Figure 6). This electron has moved to B where it forms a 3 centers−2 electrons bond. Such a center is a bipolaron or, in the language of solid-state physics, a negative Hubbard U center.

Due to the interpenetration, these two defects are not perfectly symmetric. However, it is possible that during irradiation, isolated defects of type B negatively charged or neutral (by diffusion of the A vacancy) could be formed. In such a case, they would be symmetric. In B, the Mg atoms relaxed toward the surface and became more exposed. It is possible to speculate that the formation of these defects where Mg atoms begin to form a more metallic bond is the precursor for the phenomenon of Mg aggregation during irradiation reported by Somorjai's group.[11] The relaxed structure is shown in Figure 6. The total gain of this reconstruction is 9.0 kcal/mol per Cl defect. The energy needed to form this defect is −252.5 kcal/mol.

The Wannier function representing the localization of the electron pair of defect B is shown in Figure 5b. It is delocalized between the 3 Mg atoms surrounding defect B and extends out of the plane ,thus compensating the lack of a Cl^- ion.

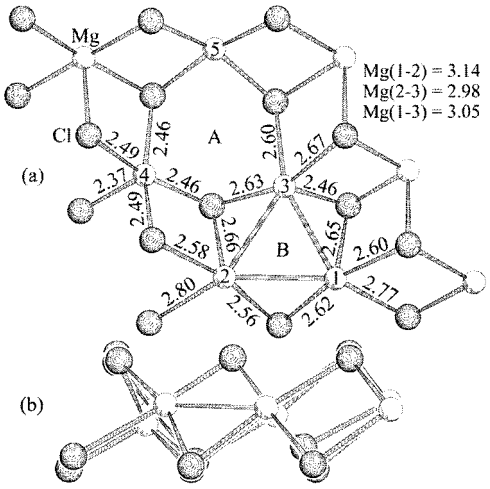

Figure 6. Relaxed $MgCl_2$ (001) monolayer with a $Cl^{\cdot}$ di-vacancy. The major structural changes upon relaxation are indicated. (a) *ab* plane. (b) *ac* plane. Distances are given in Å. Mg(5) structural environment is identical to that for Mg(4). A and B correspond to the position of the removed atoms. Relaxation energy = 9.0 kcal/mol per defect.

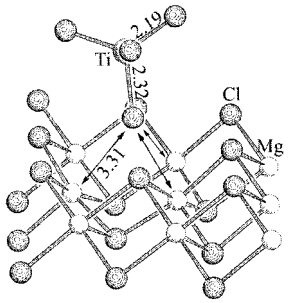

Figure 7. Relaxed structure resulting from the reaction of a $TiCl_4$ molecule on a $MgCl_2$ (001) monolayer with a Cl^- mono-vacancy. Distances are given in Å.

3. $TiCl_4$ Chemisorbtion on the Active Surfaces

3.1. $TiCl_4$ Deposition on $MgCl_2$ (001) Surface with a Cl^- Vacancy. We simulate the deposition of the catalyst by introducing a molecule of $TiCl_4$ in the vicinity of the activated surface. A CPMD simulation was performed, first without temperature control. In a second step the ion temperature was increased up to 330 K to test the stability of the arrangement. The final arrangement was optimized and is shown in Figure 7.

One of the Cl atoms of the $TiCl_4$ molecule (Cl(a)) occupies the Cl^- surface vacancy. The distances obtained between this atom and the three undercoordinated Mg of the surface are 3.31 Å. They are 30% longer than the Mg−Cl distances in bulk $MgCl_2$ and correspond to substantial interactions. These interactions stabilized the defective surface. The bonding energy of the $TiCl_4$ moiety onto the surface is 22.6 kcal/mol. A small stretching of the Mg−Cl bonds in the vicinity of the defect is observed. The bonds in apical position relative to Cl(a) are lengthened by 0.04 Å compared to that of the relaxed surface with a Cl^- vacancy. The rest of the layer is left unchanged by the $TiCl_4$ chemisorbtion. The $TiCl_4$ molecule is also affected, since Cl(a) has changed status from terminal to bridging. The distance between the metal center and Cl(a) was lengthened from 2.21 to 2.32 Å and the tetrahedral arrangement of the Ti atom distorted by shortening the three other Ti−Cl distances by 0.02 Å.

A CPMD simulation of 0.5 ps was performed to test the stability of this arrangement. The temperature was first brought

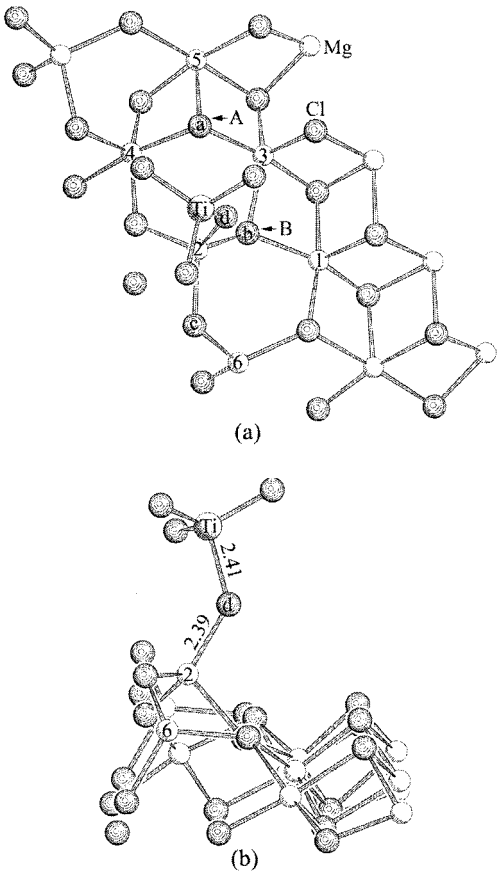

Figure 8. Relaxed structure resulting from the reaction of a $TiCl_4$ molecule on a $MgCl_2$ (001) monolayer with a Cl^- di-vacancy. (a) *ab* plane. (b) *ac* plane. Distances are given in Å. The lines correspond to the configuration of the clean di-vacancy shown in Figure 3.

to 330 K, and then the system was allowed to evolve without control. The total energy was conserved during the simulation; the instantaneous kinetic energy fluctuated between 300 and 350 K. The surface was stable during the dynamic. The dynamical motion of Cl(a) consisted of passing from an equidistant position between the 3 Mg atoms and an asymmetric one where it is closer to one of the magnesiums (typically 2.58 Å).

3.2. $TiCl_4$ Deposition on $MgCl_2$ (001) Surface with a Cl^- Di-vacancy. A CPMD simulation was performed to simulate the deposition of the $TiCl_4$ catalyst by introducing one molecule in the vicinity of the activated surface. It should be noted that the same result was obtained by putting $TiCl_4$ onto the surface in such a way that two Cl atoms of $TiCl_4$ occupied the defect sites A and B. The ion temperature was increased up to 330 K, and then the system was allowed to evolve without control.

At an early stage of the simulation, a bond was created between a Cl atom of $TiCl_4$ moiety and the undercoordinated Mg(2) atom. This occurred by an outward displacement of the Mg atom, dragging along 3 Cl atoms, two of them coming from the lower part of the layer (Cl(a), Cl(b)). This created a displacement of defects to the bottom of the layer, since these Cl atoms moved to the positions of the initial sites A and B. These structural changes in the Mg−Cl network lead to a global reorganization of the layer.

Once the arrangement was stable for 0.5 ps (no breaking and creation of bonds), it was optimized. The relaxed structure is shown Figure 8. In the relaxed structure, Mg(2) is in a tetrahedral environment of Cl atoms above the middle plane of the layer. Mg(1), Mg(3), and Mg(4) remain in an undercoordinated octahedral environment, and the position of the unoccupied site has changed from the top to the bottom of the layer. The atom Mg(5) is now surrounded by 6 Cl atoms. Cl(c) was dragged along by the motion of Mg(2) toward the surface. The cohesion of the layer is maintained by Mg(6) which adopted a tetrahedral environment, lying above the middle plane formed by the rest of the Mg atoms.

The Ti atom is in a tetrahedral environment of Cl atoms. Cl(d) which connects the catalyst and the surface is separated by 2.41 Å from the Ti atom, and by 2.39 Å from Mg(2), forming an angle of 135°. The bonding energy of the $TiCl_4$ moiety onto the surface is 53.0 kcal/mol.

3.3. $TiCl_4$ Deposition on $MgCl_2$ (001) Surface with a $Cl^\cdot$ Vacancy. As discussed earlier, on this surface there is an unpaired electron localized at the vacancy site. Close to this surface we placed a $TiCl_4$ molecule. Due to the radical nature of this defect, a spin-polarized calculation was necessary. We could not apply the standard Car−Parrinello molecular dynamics because the small HOMO−LUMO gap led to nonadiabatic behavior.[25] For this reason, we used Born−Oppenheimer dynamics. The layer proved to be very reactive. In effect, one of the chlorines of the $TiCl_4$ moiety moved in to fill the vacancy, thus forming a perfect surface, while the remaining $TiCl_3^\cdot$ radical flew away from the surface.

3.4. $TiCl_4$ Deposition on $MgCl_2$ (001) Surface with a $Cl^\cdot$ Di-vacancy. The most striking result was obtained for the $Cl^\cdot$ di-vacancy. We made two runs with different initial conditions. In one, we placed the $TiCl_4$ molecule in such a way that one of its Cl atoms was pointing toward the A defect and a second one toward B (see Figure 6). In the second simulation, we placed a $TiCl_4$ molecule above the surface and the initial Ti velocity was orientated toward the surface. In this case, eight atoms of the slab far from the defect were fixed in order to avoid a rigid surface translation.

The final results of both simulations were the same. A Cl^- ion of the $TiCl_4$ molecule occupied the A vacancy, annihilating the defect. The positively charged $TiCl_3^+$ then moved toward the closest Mg atom of the B defect, forming an intermetallic bond. A massive reconstruction followed this reaction. The Mg atom bonded to the Ti center moved toward the surface. Finally, a Cl^- went to the position of the B site, partially reconstructing the $MgCl_2$ network. The final result is a stabilization of the MgTi bond in the configuration shown in Figure 9.

The Ti−Mg(3) bond is 2.88 Å. The coordination arrangement around the Ti is tetrahedral, slightly flattened on the face formed by the 3 Cl atoms (Cl−Ti−Cl = 116°) and elongated along the Mg−Ti direction (Mg−Ti−Cl = 101°). This is due to the inhomogeneity of the nature and the lengths of the bonds around the metal atom, a metal−metal bond for Ti−Mg on one hand, and ionic interaction for Ti−Cl on the other. The Mg(3) atom is bonded to the surface through 3 Mg−Cl contacts of 2.54, 2.55, and 2.49 Å. Mg(1) and Mg(2) are left undercoordinated, with 5 Mg−Cl contacts in a square-based pyramidal arrangement.

The diabatic homogeneous dissociation energy of the Mg−Ti bond is 34.1 kcal/mol. The study of the Wannier function helps to visualize this bond. One relatively delocalized function is spread between the Mg and the Ti atoms, as shown in Figure 10, and has a $dz^2 + pz$ character.

The stability of this arrangement was tested by performing a CPMD simulation similar to the one in 3.1. For this test, none of the atoms was fixed. Apart from the normal thermal displacement of the atoms, the structure can be considered as unchanged and stable at 330 K. The frequency calculation

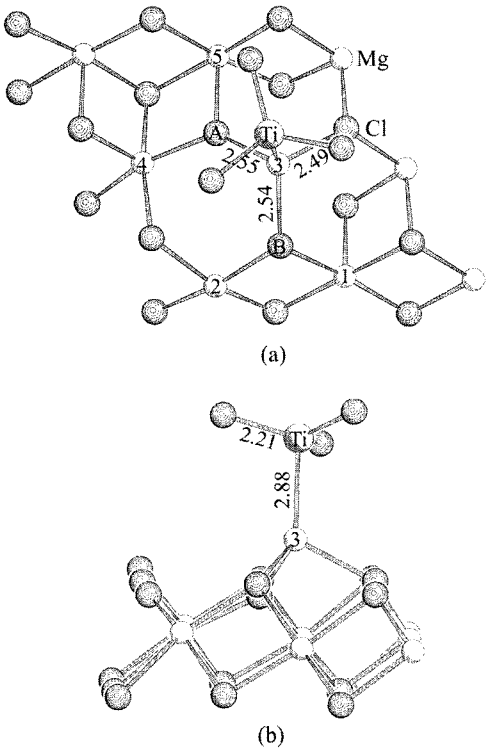

Figure 9. Relaxed structure resulting from the reaction of a $TiCl_4$ molecule on a $MgCl_2$ (001) monolayer with a $Cl^{\cdot}$ di-vacancy. (a) *ab* plane. (b) *ac* plane. Distances are given in Å. A and B are the initial positions of the defects (cf. Figure 5).

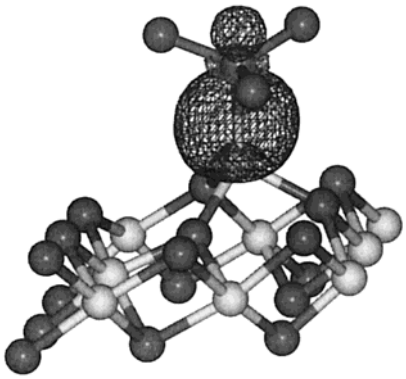

Figure 10. Contour plot of the Wannier function localized between Ti and Mg(3) of the structure shown in Figure 9. Contour values are 0.2 $(e/bohr^3)^{1/2}$.

performed on this optimized arrangement showed no negative frequency. The maximum vibration is found at 754 cm^{-1} and corresponds to a concerted motion of the Mg atoms.

Conclusion

In this article, we described the geometrical and the electronic structure of point defects on the $MgCl_2$ (001) surface. For each structure studied, the bonding properties of the atoms far from the defects are unchanged by their presence. This local nature of the reorganization upon creation of vacancies ensures the stability of those surfaces.

We showed that in the case of F-centers, the extra electrons sit between three Mg atoms. The electronic relaxation occurring to form these "metallic" bonds could be a precursor for the phenomenon of Mg aggregation that Magni et al. pointed out after irradiation of (001) surfaces.[11]

We considered the interaction of $TiCl_4$ with these defects. We found that the Ti center is bound to the Cl^- vacancy surface by 22.6 kcal/mol but is unlikely to survive the harsh environment of a catalytic process.

More promising are the complexes shown in Figures 8 and 9, which originate in the reaction of a $TiCl_4$ molecule and Cl^- and $Cl^{\cdot}$ di-vacancy surfaces, respectively. The catalytic properties of these centers will be considered in a further publication.

Acknowledgment. We thank Dr Mauro Boero and Prof. Marco Bernasconi for helpful discussions and Dr. David M. Benoit for technical help.

References and Notes

(1) (a) Ziegler, K.; Holzkamp, E.; Breil, H.; Martin, H. *Angew. Chem* **1954**, *67*, 541. (b) Natta, G. *Macromol. Chem.* **1955**, *16*, 213

(2) See for example: (a) Barbé, P. C.; Cecchin, G.; Noristi, L. *Adv. Pol. Sci.* **1987**, 81, 1. (b) Somorjai, G. A. *Introduction to Surface Chemistry and Catalysis*; Wiley and Sons: New York, 1994. (c) Kaminsky, W.; Arndt, M. Ziegler−Natta Polymerization. In *Handbook of Heterogeneous Catalysis*; Wiley-VCH: Weinheim, 1997; Vol. 5, p 2405. (d) *Progress and Development of Catalytic Olefin Polymerization*; Sano, T., Uozumi, T., Nakatani, H., Terano, M., Eds; Technology and Education Pubs.: Tokyo, 2000.

(3) See for example: (a) Lin, J. S.; Catlow, R. A. *J. Mater. Chem.* **1993**, *3*, 1217. (b) Puhakka, E.; Pakkanen, T. T.; Pakkanen, T. A. *Surf. Sci.* **1995**, *334*, 289. (c) Gale, J. D.; Catlow, C. R. A.; Gillan, M. J. *Top. Catal.* **1999**, *9*, 235. (d) Monaco, G.; Toto, M.; Guerra, G.; Corradini, P.; Cavallo, L. *Macromolecules* **2000**, *33*, 8953. (e) Martinsky, C.; Minot, C.; Ricart, J. M. *Surf. Sci.* **2001**, *490*, 237.

(4) (a) Boero, M.; Parrinello, M.; Terakura, K. *J. Am. Chem. Soc.* **1998**, *120*, 2746. (b) Boero, M.; Parrinello, M.; Terakura, K. *Surf. Sci.* **1999**, *438*, 1. (c) Boero, M.; Parrinello, M.; Weiss, H.; Hueffer, S. *J. Am. Chem. Soc.* **2000**, *122*, 501. (d) Boero, M.; Parrinello, M.; Weiss, H.; Hueffer, S. *J. Phys. Chem. A* **2001**, *105*, 5096.

(5) Freund, H.-J. *Angew. Chem., Int. Ed. Engl.* **1997**, *36*, 452.

(6) Kim, S. H.; Somorjai, G. A. *J. Phys. Chem. B* **2001**, *105*, 3922.

(7) Kim, S. H.; Somorjai, G. A. *Appl. Surf. Sci.* **2000**, *161*, 333.

(8) Kim, S. H.; Tewell, C. R.; Somorjai, G. A. *Langmuir* **2000**, *16*, 9414.

(9) Kim, S. H.; Somorjai, G. A. *J. Phys. Chem. B* **2000**, *104*, 5519.

(10) Magni, E.; Koranyi, T.; Somorjai, G. A. *Langmuir* **2000**, *16*, 8113.

(11) Magni, E.; Somorjai, G. A. *Surf. Sci.* **1996**, *345*, 1.

(12) Magni, E.; Somorjai, G. A. *J. Phys. Chem. B* **1996**, *100*, 14786.

(13) Magni, E.; Somorjai, G. A. *Surf. Sci.* **1997**, *377*, 824.

(14) Magni, E.; Somorjai, G. A. *Catal. Lett.* **1995**, *35*, 205.

(15) Somorjai, G. A. *J. Phys. Chem. B* **1998**, *102*, 8788.

(16) (a) Kohn, W.; Sham, L. *J. Phys. Rev.* **1965**, *140*A, 1133. (b) Jones, R. O.; Gunnarsson, O. *Rev. Mod. Phys.* **1989**, *61*, 689.

(17) Becke, A. D. *Phys. Rev. A* **1988**, *38*, 3098. (a) Lee, C.; Yang, W.; Parr, R. G. *Phys. Rev. B* **1988**, *37*, 785.

(18) (14) Trouiller, N.; Martins, J. L. *Phys. Rev. B* **1991**, *43*, 1993.

(19) Louie, S. G.; Froyen, S.; Cohen, M. L. *Phys. Rev. B* **1982**, *26*, 1738.

(20) CPMD, J. Hutter et al. MPI für Festkörperforschung and IBM Zurich Research Laboratory, 1990−2001.

(21) Doorepaal, J. *J. Appl. Crystallogr.* **1984**, *17*, 483.

(22) Car, R.; Parrinello, M. *Phys. Rev. Lett.* **1985**, *55*, 2471.

(23) Bersuker, I. B. *Chem. Rev.* **2001**, *101*, 1067.

(24) Wannier, G. H. *Phys. Rev.* **1937**, *52*, 191; Marzari, N.; Vanderbilt, D. *Phys. Rev. B.* **1997**, *56*, 12847; Silvestrelli, P. *Phys. Rev. B* **1998**, *59*, 9703.

(25) Marx, D.; Hutter, J. Ab Initio molecular dynamics: Theory and Implementation. In *Modern Methods and Algorithms of Quantum Chemistry*, NIC Series; Grotendorst, J., Ed.; John von Neumann Institute for Computing, Jülich, 2000; Vol. 1, pp 301−449.